

ASIA-PACIFIC METROLOGY PROGRAMME
10 MPa HYDRAULIC GAUGE PRESSURE BILATERAL SUPPLEMENTARY COMPARISON
Comparison Identifier: **APMP.M.P-S5**

**Final Report on Bilateral Supplementary Comparison
APMP.M.P-S5 in Hydraulic Gauge Pressure
from 1 MPa to 10 MPa**

February 13, 2016

Jin Yue¹, Yuanchao Yang¹, Wladimir Sabuga²

¹ NIM: National Institute of Metrology, 18 Beisanhuan donglu, chaoyang district,
Beijing, China

² PTB: Physikalisch-Technische Bundesanstalt, Bundesallee 100, 38116 Braunschweig,
Germany

Abstract

This report summarizes the results of the Asia-Pacific Metrology Programme (APMP) supplementary comparison APMP.M.P-S5 for hydraulic gauge pressure in the range of 1 MPa to 10 MPa, which is a bilateral comparison carried out at the National Institute of Metrology, China (NIM) and the Physikalisch-Technische Bundesanstalt, Germany (PTB) during the period June 2014 to June 2015. NIM piloted the comparison and provided the transfer standard, which was a piston-cylinder assembly (PCA) of 1 cm² nominal effective area built in a hydraulic pressure balance manufactured by Fluke Corporation. The laboratory standards of NIM and PTB are both hydraulic pressure balances equipped with PCAs, of which the nominal effective area is 1 cm² for NIM and 5 cm² for PTB. The results of the comparison successfully demonstrated that the hydraulic gauge pressure standards of NIM and PTB in the range of 1 MPa to 10 MPa are equivalent within their claimed uncertainties.

Contents:	Page
1. Introduction	1
2. Description of the Laboratory Standards.....	1
2.1 NIM Laboratory Standard	1
2.2 PTB Laboratory Standard	2
3. Transfer standard.....	4
4. Time schedule	5
5. Calibration methods	6
5.1 NIM calibration method	6
5.2 PTB calibration method	8
6. Analysis of the reported data	9
6.1 Data reduction	9
6.2 Uncertainty evaluation	11
7. Results and discussions	15
7.1 Evaluation of degree of equivalence	15
7.2 Zero-pressure effective area and distortion coefficient	17
8. Conclusions and discussion	19
Acknowledgements.....	19
References	19

1. Introduction

At the CCM High Pressure Working Group meeting at the Bureau International des Poids et Mesures (BIPM) in February 2014, the National Institute of Metrology (NIM), China, and the Physikalisch-Technische Bundesanstalt (PTB), Germany, agreed to carry out a bilateral supplementary comparison (SC) of their hydraulic gauge pressure standards in the range up to 10 MPa. The comparison in this pressure range is motivated by the fact that, in both National Metrology Institutes (NMIs), their 10 MPa pressure standards provide traceability in terms of zero pressure effective area to all hydraulic pressure balances operated above 10 MPa.

This SC is identified as APMP.M.P-S5 in the BIPM key comparisons database.

The pilot laboratory of the SC is NIM, which also has provided a transfer standard (TS) for this comparison.

2. Description of the Laboratory Standards

2.1 NIM Laboratory Standard

The NIM laboratory standard (LS) used in this SC was a 10 MPa pressure balance with a piston-cylinder assembly (PCA) identified as 66501, which is one of a group of 5 nominal identical PCAs with cross-section areas of 1 cm². The working fluid is a mixture of paraffin and transformer oil. The zero-pressure effective areas of the 5 PCAs were determined from dimensional measurements and inter-comparisons [1]. The value of the distortion coefficient (λ) was calculated by the Lamé theory using equation (1) based on the PCA's dimensions and the elastic constants of its material.

$$\lambda = \frac{3\mu_p - 1}{2E_p} + \frac{1}{2E_c} \left(\frac{R_c^2 + R_0^2}{R_c^2 - R_0^2} + \mu_c \right) \quad (1)$$

where E_p , E_c , μ_p and μ_c are Young's modulus and Poisson's ratio of the piston and cylinder, respectively, and R_c and R_0 are the outer and inner radii of the cylinder. The elastic constants, Young's modulus (E) and Poisson's ratio (μ), for the piston and cylinder are the same and taken as: $E = 210$ GPa and $\mu = 0.29$. The effective area and distortion coefficient of the PCA 66501 were also measured against a pneumatic piston gauge. The detailed properties of the NIM LS are summarized in Table 1. All uncertainties in this report refer to standard uncertainty unless noted otherwise.

Table 1. Details of the NIM laboratory standard

Pressure balance	Manufacturer of base and piston-cylinder	NIM, PCA SN: 66501
	Measurement range in MPa	1 ~ 10
	Operation mode	Simple free-deformation
	Total mass in kg	100
	Typical relative uncertainty of mass pieces in 10^{-6}	1.6
	Working fluid	20% paraffin and 80% transformer oil (volume)
	Surface tension of the fluid in mN/m	24.9
	Thermometer	PRT 100, SN: C0199
	Piston rotation	By hand, free rotation
	Piston rotation speed in rpm	15 ~ 25
PCA	Material of piston and cylinder	Steel
	Linear thermal expansion coefficient (α) of piston and cylinder in $^{\circ}\text{C}^{-1}$	1.2×10^{-5}
	Zero-pressure effective area (A_0) at ref. temp. in cm^2	1.0072065
	Relative uncertainty of A_0 in 10^{-6}	9.0
	Reference temperature in $^{\circ}\text{C}$	20
	Pressure distortion coefficient (λ) in MPa^{-1}	3.73×10^{-6}
	Uncertainty of λ in MPa^{-1}	0.62×10^{-6}
Ambient conditions	Local gravity (g) in m/s^2	9.801245
	Relative uncertainty of g in 10^{-6}	0.2
	Atmospheric temperature measurement	Testo, 608-H1
	Range of atmospheric temperature in $^{\circ}\text{C}$	19.5 ~ 21.3
	Atmospheric humidity measurement	Testo, 608-H1
	Range of atmospheric humidity in %	43.1 ~ 61.6
	Atmospheric pressure measurement	Paroscientific, 745
	Range of atmospheric pressure in hPa	1006.2 ~ 1026.3

2.2 PTB Laboratory Standard

The PTB laboratory standard (LS) used in this SC was the 1 GPa pressure balance [2] equipped with a 10 MPa piston-cylinder assembly (PCA) identified by serial no. 278. Details of the LS and the measurement conditions are presented in Table 2.

Table 2. Laboratory standard and measurement conditions

Manufacturer	Pressure balance – Harwood, 1.4 GPa model, PTB modified Piston-cylinder – DHI, special design, ser. no. 278
Measurement range in MPa	0.25 – 10
Weights manufacturer	Harwood
Weights total mass in kg	500
Typical relative uncertainty of mass pieces in 10^{-6}	0.51
Piston rotation	By motor
Piston rotation speed in rpm	8
Material of piston	WC + 6% Co, VISTA 'VM-6M'
Material of cylinder	WC + 6% Co, VISTA 'VM-6M'
Operation mode, free-deformation (FD) or controlled-clearance (CC)	FD
Thermometer	PRT 100, PTB MM–Nr. A3-174
Zero-pressure effective area (A_0) at reference temperature in cm^2	4.902617
Relative uncertainty of A_0 in 10^{-6}	5.0
Pressure distortion coefficient (λ) in MPa^{-1}	$1.20 \cdot 10^{-6}$
Uncertainty of λ in MPa^{-1}	$0.10 \cdot 10^{-6}$
Linear thermal expansion coefficient of piston (α_p) in $^{\circ}\text{C}^{-1}$	$4.5 \cdot 10^{-6}$
Linear thermal expansion coefficient of cylinder (α_c) in $^{\circ}\text{C}^{-1}$	$4.5 \cdot 10^{-6}$
Reference temperature (t_0) in $^{\circ}\text{C}$	20
Local gravity (g) in m/s^2	9.812533
Relative uncertainty of g in 10^{-6}	0.54
Atmospheric temperature measurement	PRT 100, PTB MM–Nr. A3-138, Heraeus Kn 3026
Uncertainty of the atmospheric temperature in $^{\circ}\text{C}$	0.20
Atmospheric RH measurement	Combined Transmitter, PTB MM–Nr. A3-190, Vaisala PTU303
Uncertainty of the RH in %	30
Atmospheric pressure measurement	Digital Pressure Transducer, PTB MM–Nr. A3-045, Setra 370
Uncertainty of the atmospheric pressure in hPa	0.10

The zero-pressure effective area (A_0) of this assembly is traceable to SI units through dimensional measurements carried out on three nominally identical 5 cm^2 10 MPa PCAs 278, 279 and 280 [3] with a following synchronisation of the dimensional effective areas by cross-float measurements [4]. The last actualisation of the A_0 value is dated by April 2012.

The value of the distortion coefficient (λ) was calculated by the Lamé theory using PCA's dimensions and the elastic constants of the PCA material. The elastic constants, the Young modulus (E) and the Poisson coefficient (μ) were measured on the material of the PCA, i.e. coming from the same material batch, using the Resonant Ultrasound Spectroscopy [5] with the following results:

$E = (627.35 \pm 0.45)$ GPa and $\mu = 0.2113 \pm 0.0005$. The uncertainty of λ is an experience value based on analyses in which the Lamé theory was compared with more sophisticated methods such as Finite Element Method [6–8].

The 5 cm² 10 MPa PCAs described above have never been used so far in any international comparison directly, but provide traceability for all other PTB hydraulic pressure standards operated at higher pressures, many of which have successfully participated in several CCM, EURAMET, COOMET and APMP comparisons.

3. Transfer standard

The transfer standard (TS) provided by NIM was a piston-cylinder assembly of 1 cm² nominal effective area with serial number 1122. It was built in a hydraulic pressure balance PG7307 equipped with a mass loading bell, all parts having been manufactured by Fluke Corporation, DH Instruments Division, USA, being parts of the transfer standard. The TS was a controlled-clearance piston gauge. However in this SC, it was operated in the free-deformation mode, leaving the controlled-clearance pressure port opening to the atmosphere.

For loading the piston, NIM and PTB used their own mass sets. The NIM mass set was 100 kg in total mass with 10 kg main weights. The PTB mass set was identified by g23ma2, whose masses of the main 5 kg weights were known with a relative uncertainty of $5.0 \cdot 10^{-7}$.

The details of all the relevant technical data of TS were given in the Technical Protocol of this SC [9], and are summarized in Table 3.

Table 3. Details of the transfer standard

Piston-cylinder assembly	Model: PC-7307-100, SN: 1122
Instrument platform	Model: PG7307, SN: 687
Mass loading bell	Model: PG7000, SN: 834
Measurement range in MPa	1 ~ 10
Operation mode	Simple free-deformation
Working fluid	Di(2-ethylhexyl) sebacate (DHS)
Surface tension of the fluid in mN/m	31.2
Piston rotation	Starting by motor or by hand, then freely rotating
Piston rotation speed in rpm	15 ~ 25
Material of piston and cylinder	Tungsten carbide
Linear thermal expansion coefficient (α) of piston and cylinder in °C ⁻¹	4.5×10^{-6}

The temperature of the TS PCA was measured with a platinum resistance thermometer (PRT) built in the PG7307 platform and was displayed on the PG terminal. At the pilot institute, the PRT had been calibrated in the temperature range (18.0 ~ 22.0) °C. The calibration results are shown in Table 4.

Table 4. Calibration results of the PRT in the transfer standard

Reference (°C)	PRT (°C)	$U(k=2)$ (°C)
17.998	17.98	0.02
18.994	18.98	0.01
19.990	19.98	0.01
20.988	20.97	0.01
21.986	21.97	0.01

4. Time schedule

The comparison was scheduled to start the measurements in June 2014. In order to check the stability of the TS, the whole measurement phase lasted almost one year, which included 4 calibrations at NIM and 1 calibration at PTB. For each calibration, 5 runs measurement data was collected, except for the first calibration at NIM, which collected 6 runs data.

The TS arrived at PTB from NIM on 14 November 2014, and the measurements at PTB were carried out between 2 and 8 December 2014. Then it was sent back to NIM on 18 December 2014.

The actual chronology of the measurements was presented in Table 5.

Table 5. Chronology of the measurements

Laboratory	Calibration Start Date	Calibration End Date
NIM 1	25 June 2014	11 July 2014
NIM 2	10 September 2014	17 September 2014
PTB	2 December 2014	8 December 2014
NIM 3	4 February 2015	12 February 2015
NIM 4	1 June 2015	5 June 2015

5. Calibration methods

According to the protocol [9], it was required that each laboratory calibrate the effective area of the TS in the pressure sequence (1, 2, 3, 4, 5, 6, 7, 8, 9, 10, 10, 9, 8, 7, 6, 5, 4, 3, 2, 1) MPa for five cycles with each cycle taken on a different day. The specific calibration methods used in NIM and PTB are described in the following sections respectively.

5.1 NIM calibration method

Since the NIM LS used a different working fluid from the TS, a Visible Level Interface (VLI, a product of DHI, Fluke), as shown in Figure 1, was connected in the manifold between the LS and TS to separate the two kinds of fluid.

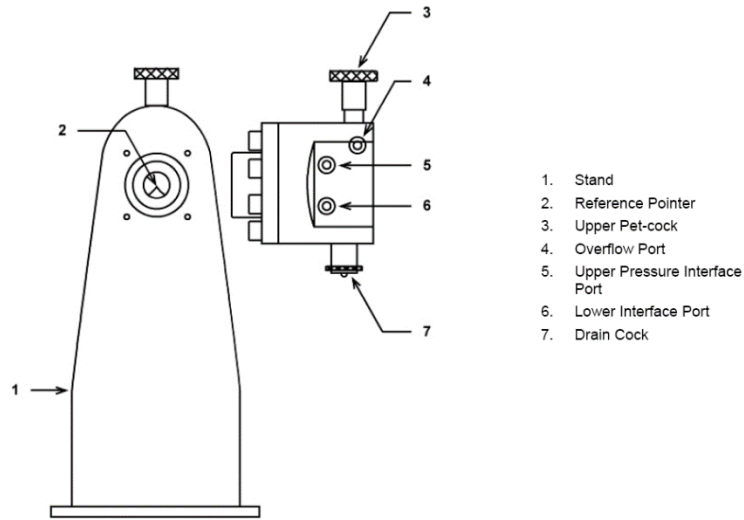


Figure 1. Visible level interface to separate working fluids

Considering the larger density of DHS than the mixture oil, DHS was firstly introduced into the VLI until its surface reached the Reference Pointer, then the VLI was full-filled with the mixture oil and sealed. The interface was maintained at the Reference Pointer and clearly visible during one measurement cycle. After each measurement cycle, the fluid in the VLI was drained away, and the VLI was refilled before a new cycle.

Cross-float measurements were carried out at each target pressure. The fall-rate method was used to judge the equilibrium. The effective area of TS determined from a particular measurement (A_p) referred to 20 °C was calculated using equation (2) as described in the Technical Protocol [9]:

$$A_p = \frac{\sum_i m_i g \left(1 - \frac{\rho_a}{\rho_i} \right) + 2\sigma \sqrt{\pi A_{0,\text{nom}}}}{p [1 + (\alpha_p + \alpha_c)(t - t_0)]} \quad (2)$$

- m_i — True mass of the piston, the weight carrier, the mass pieces and the trim masses loaded on the TS, kg
- ρ_i — Density of the part with mass m_i , kg/m³
- ρ_a — Air density, kg/m³

g	—	Local gravity acceleration, m/s ²
σ	—	Surface tension of the TS working fluid, N/m
$A_{0,nom}$	—	Nominal effective area of the TS, m ²
p	—	Pressure generated by the LS at the TS reference level, Pa
α_p, α_c	—	Thermal expansion coefficients of the piston and cylinder materials of the TS, respectively, °C ⁻¹
t	—	Temperature of the TS, °C
t_0	—	Reference temperature, 20 °C

The p was determined by equation (3):

$$p = \frac{\sum_i m_{i,LS} g \left(1 - \frac{\rho_a}{\rho_{i,LS}}\right) + 2\sigma_{LS} \sqrt{\pi A_{0,LS}}}{A_{0,LS} \left[1 + (\alpha_{p,LS} + \alpha_{c,LS})(t_{LS} - t_0)\right] (1 + \lambda_{LS} p)} + (\rho_{LS} - \rho_a)gh_1 + (\rho_{TS} - \rho_a)gh_2 \quad (3)$$

in which

$m_{i,LS}$	—	True mass of the piston, the weight carrier and the mass pieces loaded on the LS, kg
$\rho_{i,LS}$	—	Density of the part with mass m_i , kg/m ³
σ_{LS}	—	Surface tension of the LS working fluid, N/m
$A_{0,LS}$	—	Nominal effective area of the LS, m ²
$\alpha_{p,LS}, \alpha_{c,LS}$	—	Thermal expansion coefficients of the piston and cylinder materials of the LS, respectively, °C ⁻¹
t_{LS}	—	Temperature of the LS, °C
t_0	—	Reference temperature, 20 °C
λ_{LS}	—	Pressure distortion coefficient of the LS, MPa ⁻¹
ρ_{LS}, ρ_{TS}	—	Density of the working fluids of the LS and TS, respectively, kg/m ³
h_1	—	Height difference between the reference level of the LS and VLI, m
h_2	—	Height difference between the reference level of the VLI and TS, m

and all other symbols as defined before.

Although the interface in the VLI was clearly visible, the diffusion between the two kinds of fluid was inevitable and the density of the fluids might be changed during the measurement in a manner we didn't know. To reduce this effect on the head correction, the height difference between the LS and the VLI ($h_1 = h_{LS} - h_{VLI}$), also between the VLI and the TS ($h_2 = h_{VLI} - h_{TS}$), was minimized. In practice, h_1 was measured to be 0.30 mm, while h_2 was 1.24 mm. Their uncertainty was estimated to be 0.5 mm.

The density of the working fluid of the LS was $861.8 \times (1 \pm 0.02)$ kg/m³. The density of DHS, the working fluid of the TS, in dependence on pressure (p) and temperature (t) was calculated using equation (4) as provided in the Technical Protocol [9]:

$$\rho_{TS} = [912.7 + 0.752(p/\text{MPa}) - 1.65 \cdot 10^{-3}(p/\text{MPa})^2 + 1.5 \cdot 10^{-6}(p/\text{MPa})^3] \times [1 - 7.8 \cdot 10^{-4}(t/^\circ\text{C} - 20)] \times (1 \pm 0.01) \text{ kg/m}^3 \quad (4)$$

The surface tension coefficient of the working fluid of the LS was measured to be $24.9 \times (1 \pm 0.1)$ mN/m. And for the DHS, it was $31.6 \times (1 \pm 0.1)$ mN/m, which was consistent with the value, $31.2 \times (1 \pm 0.05)$ mN/m, provided in the Technical Protocol [9].

The air density was calculated from the temperature, pressure and humidity of the ambient air using equation (5):

$$\rho_a = \frac{0.34848p - 0.009(RH) \times \exp(0.062t)}{273.15 + t} \quad (5)$$

where

- p — Atmospheric pressure, hPa
- RH — Relative humidity, %
- t — Air temperature, °C

5.2 PTB calibration method

Prior to pressure measurements, magnetisation of TS was measured and found to be $5 \cdot 10^{-5}$ Tesla at piston and $5 \cdot 10^{-5}$ Tesla at cylinder. The piston fall rates (v_f) were measured as:

p / MPa	$v_f / (\text{mm}/\text{min})$
1	0.003
5	0.010
10	0.021

All measurements were performed by a direct cross-float of TS against LS using di(2)-ethyl-hexyl-sebacate (DHS) as the pressure transmitting medium in both standards. The density was calculated using equation (4), and the surface tension was $31.2 \times (1 \pm 0.05)$ mN/m.

At each pressure, LS and TS were cross-floated using the fall rates of both pistons as an equilibrium criterion. To reach the equilibrium, trim masses were applied only to LS, whereas TS was operated only with the standard 5 kg weights set.

TS was installed with keeping the height difference between LS and TS (h) minimal. The height difference, temperatures of LS and TS (t_{LS} and t_{TS}) as well as ambient conditions are summarised in Table 6.

Table 6. Experimental and ambient conditions

Height difference between laboratory standard (LS) and TS (h , positive if LS is higher than TS) in mm	-0.48
Uncertainty of h in mm	0.37
Range of temperature of LS (t_{LS}) in °C	19.49 – 20.12
Range of temperature of TS (t_{TS}) in °C	19.84 – 20.46
Range of ambient temperature (t_{amb}) in °C	19.30 – 19.84
Range of ambient pressure (p_{amb}) in hPa	1007.58 – 1014.88
Range of ambient relative humidity (RH_{amb}) in %	30 – 43

The pressure measured in the reference level of TS (p) and the pressure dependent effective area of TS (A_p) were calculated from the well-known formulae:

$$p = \frac{g \sum m_{i,LS} (1 - \rho_a / \rho_{m_{i,LS}}) + 2\pi r_{LS} \sigma}{A_{0,LS} [1 + (\alpha_{p,LS} + \alpha_{c,LS})(t_{LS} - t_0)] (1 + \lambda_{LS} p)} + g(\rho_l - \rho_a)h \quad (6)$$

$$A_p = \frac{g \sum m_i (1 - \rho_a / \rho_{m_i}) + 2\pi r \sigma}{p [1 + (\alpha_p + \alpha_c)(t - t_0)]}, \quad \text{where} \quad (7)$$

r is piston radius,

h is height difference between LS and TS,

and all other symbols as defined in 5.1. Quantities with subscript "LS" refer to properties of LS, all other quantities are properties of TS or parameters which are common for both LS and TS.

The air density was calculated from the temperature, pressure and humidity of the ambient air using the equation given in [10].

6. Analysis of the reported data

6.1 Data reduction

NIM reported 4 calibration results and PTB reported 1 calibration result. Each calibration result contained the effective areas of the TS in the pressure sequence (1, 2, 3, 4, 5, 6, 7, 8, 9, 10, 10, 9, 8, 7, 6, 5, 4, 3, 2, 1) MPa with 5 repeated measurements. The results can be expressed as A_{p_i,j,NIM_k} for NIM and $A_{p_i,j,PTB}$ for PTB, where p_i are the pressure points ($i=1,2,\dots,10$), $j(=1,2,\dots,10)$ enumerates A_{p_i} values at p_i and $k(=1,2,3,4)$ is the calibration time at NIM. The results of $k=2$ and 3 (before and after the measurements at PTB) were averaged and taken as the result of NIM as expressed by equation (8).

$$A_{p_i,j,NIM} = \frac{1}{2} (A_{p_i,j,NIM_2} + A_{p_i,j,NIM_3}) \quad (8)$$

The average values of A_{p_i} for each laboratory and their relative standard deviations were

calculated using equation (9) and (10), also summarized in Table 7 and 8.

$$A_{p_i} = \frac{1}{10} \sum_j A_{p_i,j} \quad (9)$$

$$\frac{s(A_{p_i})}{A_{p_i}} = \frac{1}{A_{p_i}} \sqrt{\frac{\sum_j (A_{p_i,j} - A_{p_i})^2}{10-1}} \quad (10)$$

Table 7. Summary results of NIM

Nominal pressure	Typical min. adjusted mass ¹⁾	Average of A_p , $\langle A_p \rangle$ ²⁾	Relative standard deviation of $\langle A_p \rangle$ ³⁾	Relative standard uncertainty of p ⁴⁾	Standard uncertainty of t ⁵⁾	Relative standard uncertainty of $\langle A_p \rangle$ ⁶⁾
MPa	mg	mm ²	10 ⁻⁶	10 ⁻⁶	°C	10 ⁻⁶
1	10	98.04070	2.21	11.7	0.2	12.3
2	10	98.04079	1.01	10.4	0.2	10.9
3	10	98.04097	0.93	10.2	0.2	10.7
4	10	98.04110	0.67	10.2	0.2	10.7
5	10	98.04124	0.95	10.3	0.2	10.8
6	20	98.04142	0.79	10.5	0.2	11.0
7	20	98.04154	0.54	10.7	0.2	11.2
8	20	98.04169	0.52	11.0	0.2	11.4
9	20	98.04175	0.41	11.3	0.2	11.7
10	20	98.04186	0.37	11.6	0.2	12.0

Table 8. Summary results of PTB

Nominal pressure	Typical min. adjusted mass ¹⁾	Average of A_p , $\langle A_p \rangle$ ²⁾	Relative standard deviation of $\langle A_p \rangle$ ³⁾	Relative standard uncertainty of p ⁴⁾	Standard uncertainty of t ⁵⁾	Relative standard uncertainty of $\langle A_p \rangle$ ⁶⁾
MPa	mg	mm ²	10 ⁻⁶	10 ⁻⁶	°C	10 ⁻⁶
1	20	98.04183	0.66	6.5	0.08	6.6
2	20	98.04181	0.65	5.5	0.08	5.6
3	20	98.04190	0.42	5.3	0.08	5.4
4	40	98.04195	0.50	5.2	0.08	5.3
5	40	98.04205	0.56	5.2	0.08	5.3
6	40	98.04212	0.44	5.2	0.08	5.3
7	40	98.04222	0.47	5.2	0.08	5.3
8	40	98.04231	0.51	5.2	0.08	5.3
9	50	98.04240	0.46	5.2	0.08	5.3
10	50	98.04247	0.42	5.2	0.08	5.3

¹⁾ The smallest mass adjusted on the piston of the TS to reach the equilibrium between it and the participating institute's standard;

²⁾ Average of the values measured at the same nominal pressure;

³⁾ Standard deviation of a single value;

⁴⁾ Type B uncertainty including the uncertainty of the pressure at the reference level of TS, which includes uncertainty of pressure generated by the institute's standard, of the height difference between the institute's standard and TS, of the density of the pressure transmitting medium, etc.;

⁵⁾ Type B uncertainty of the temperature measurement on TS

⁶⁾ Combined uncertainty of the mean values in ²⁾.

6.2 Uncertainty evaluation

The relative uncertainties of A_{p_i} are listed in the last column of Tables 7 and 8. They are combined uncertainties including the type A uncertainties derived from equation (10) and the type B uncertainties reported by each laboratory. The calculation of type B uncertainty is based on the ISO GUM [11]. Tables 9 and 10 present the type B uncertainty budgets at 1 MPa and 10 MPa evaluated by NIM and PTB, respectively. To calculate the output value for each input quantity, NIM used the sensitivity coefficient method while PTB used the numerical method (variation of parameters).

Table 9. NIM type B uncertainty budgets for A_{p_i} at 1 MPa and 10 MPa

Input quantity	Uncertainty	Sensitivity coefficient	$u(\langle A_p \rangle)/\langle A_p \rangle$ $\times 10^6$ at 1 MPa	$u(\langle A_p \rangle)/\langle A_p \rangle$ $\times 10^6$ at 10 MPa
m_{LS} , LS weights mass	1.6×10^{-6} rel.	1	1.6	1.6
m_{TS} , TS weights mass	1.6×10^{-6} rel.	1	1.6	1.6
ρ_{LS} , LS weights mass density	80 kg/m ³	1.9×10^{-8} kg ⁻¹ m ³	1.5	1.5
ρ_{TS} , TS weights mass density	80 kg/m ³	1.9×10^{-8} kg ⁻¹ m ³	1.5	1.5
$\sigma_{oil LS}$, surface tension of LS oil	10% rel.	$1.06 \times 10^{-5}/(p/\text{MPa})$	1.06	0.11
$\sigma_{oil TS}$, surface tension of TS oil	10% rel.	$1.06 \times 10^{-5}/(p/\text{MPa})$	1.06	0.11
$\rho_{oil LS}$, density of LS oil	2% rel.	$3 \times 10^{-6}/(p/\text{MPa})$	0.06	0.01
$\rho_{oil TS}$, density of TS oil	1% rel.	$1.1 \times 10^{-5}/(p/\text{MPa})$	0.11	0.01
h_1 , height difference between LS and VLI	0.5 mm	$8.5 \times 10^{-6}/(p/\text{MPa})$ mm ⁻¹	4.25	0.43
h_2 , height difference between VLI and TS	0.5 mm	$9 \times 10^{-6}/(p/\text{MPa})$ mm ⁻¹	4.50	0.45
α_{LS} , thermal expansion coefficient of LS	2.4×10^{-6} °C ⁻¹	0.8 °C	1.92	1.92
α_{TS} , thermal expansion coefficient of TS	9×10^{-7} °C ⁻¹	1.3 °C	1.17	1.17
t_{LS} , temperature of LS	0.1 °C	2.4×10^{-5} °C ⁻¹	2.4	2.4
t_{TS} , temperature of TS	0.2 °C	9×10^{-6} °C ⁻¹	1.8	1.8
Verticality	1 mm/m	1	0.5	0.5
Cross-float sensitivity	10 mg, 20 mg	$1 \times 10^{-7}/(p/\text{MPa})$ mg ⁻¹	1.0	0.2
$A_{0,LS}$, effective area of LS	9×10^{-6} rel.	1	9.0	9.0
λ_{LS} , distortion coefficient of LS	6.2×10^{-7} MPa ⁻¹	p MPa	0.62	6.20
Combined type B uncertainty			12.1	12.0

Table 10. PTB type B uncertainty budgets for A_{p_i} at 1 MPa and 10 MPa

Quantity	Uncertainty	$u(\langle A_p \rangle) / \langle A_p \rangle$ $\times 10^6$ at 1 MPa	$u(\langle A_p \rangle) / \langle A_p \rangle$ $\times 10^6$ at 10 MPa
g variation within 0.5 m height	$1.6 \cdot 10^{-6}$ m/s ²	0.16	0.16
Room temperature	$2.0 \cdot 10^{-1}$ °C	0.03	0
Relative humidity	$3.0 \cdot 10^{+1}$ %	0.09	0.01
DHS density	$1.0 \cdot 10^{-2}$ rel.	0.04	0
DHS surface tension	$5.0 \cdot 10^{-2}$ rel.	0.31	0.03
Height difference	$3.7 \cdot 10^{-1}$ mm	3.3	0.33
PT-100 in LS	$2.0 \cdot 10^{-2}$ °C	0.18	0.18
PT-100 in TS	$2.0 \cdot 10^{-2}$ °C	0.18	0.18
Temperature inhomogeneity	$7.1 \cdot 10^{-2}$ °C	0.64	0.64
LS thermal expansion coeff.	$9.0 \cdot 10^{-7}$ °C ⁻¹	0.46	0.29
TS thermal expansion coeff.	$9.0 \cdot 10^{-7}$ °C ⁻¹	0.01	0.14
LS distortion coefficient	$1.0 \cdot 10^{-7}$ MPa ⁻¹	0.10	1.0
LS verticality	1.0 mm/m	0.50	0.50
TS verticality	1.0 mm/m	0.50	0.50
LS piston & weight carrier mass	$2.0 \cdot 10^{-6}$ kg	0.04 ⁷⁾	0 ⁷⁾
LS piston & weight carrier density	$5.0 \cdot 10^{-2}$ g/cm ³		
TS piston & weight carrier mass	$3.5 \cdot 10^{-6}$ kg	0.31 ⁷⁾	0.03 ⁷⁾
TS piston & weight carrier density	$5.0 \cdot 10^{-2}$ g/cm ³		
LS ring weights mass	$3.9 \cdot 10^{-4}$ kg	2.2 ⁷⁾	0.53 ⁷⁾
LS ring weights density	$2.9 \cdot 10^{-2}$ g/cm ³		
TS ring weights mass	$5.0 \cdot 10^{-5}$ kg	0.26 ⁷⁾	0.17 ⁷⁾
TS ring weights density	$2.5 \cdot 10^{-2}$ g/cm ³		
LS trim masses	$3.9 \cdot 10^{-6}$ kg	0.04	0.01
LS effective area	$5.0 \cdot 10^{-6}$ rel.	5.0	5.0
Combined type B uncertainty		6.5	5.2

⁷⁾ The uncertainties of the mass and of the corresponding density are highly correlated due to the preceding weighing process in air. As uncertainty component $u(A_p)/A_p$ the resulting value from both contributing input quantities is given taking into account their correlation coefficient using the propagation of uncertainty.

The TS had been calibrated 4 times at the pilot laboratory from June 2014 to June 2015. The long-term stability of the TS can be studied using these calibration data. Table 11 presents the summary results of the 4 calibrations, including the average of A_{p_i} and their relative standard deviations obtained from each calibration.

Table 11. Summary results of the 4 calibrations at NIM

Nominal pressure	Average of A_{pi} , $\langle A_{pi} \rangle$ in mm ²				Relative standard deviation of $\langle A_{pi} \rangle$ in 10 ⁻⁶			
MPa	NIM-1 Jun. 2014	NIM-2 Sep. 2014	NIM-3 Feb. 2015	NIM-4 Jun. 2015	NIM-1 Jun. 2014	NIM-2 Sep. 2014	NIM-3 Feb. 2015	NIM-4 Jun. 2015
1	98.04081	98.04058	98.04082	98.04093	2.68	4.13	2.88	2.06
2	98.04099	98.04069	98.04090	98.04100	1.88	1.61	0.84	1.35
3	98.04107	98.04088	98.04107	98.04103	1.49	2.03	0.95	0.84
4	98.04122	98.04102	98.04119	98.04110	1.00	1.33	0.78	0.51
5	98.04132	98.04117	98.04130	98.04127	1.01	1.10	1.02	0.84
6	98.04151	98.04135	98.04149	98.04136	0.88	0.97	1.05	0.81
7	98.04160	98.04147	98.04161	98.04145	0.62	0.77	0.85	0.65
8	98.04176	98.04163	98.04174	98.04164	0.92	0.60	0.64	0.56
9	98.04176	98.04169	98.04181	98.04174	0.93	0.70	0.50	0.66
10	98.04193	98.04179	98.04194	98.04181	0.69	0.40	0.54	0.54

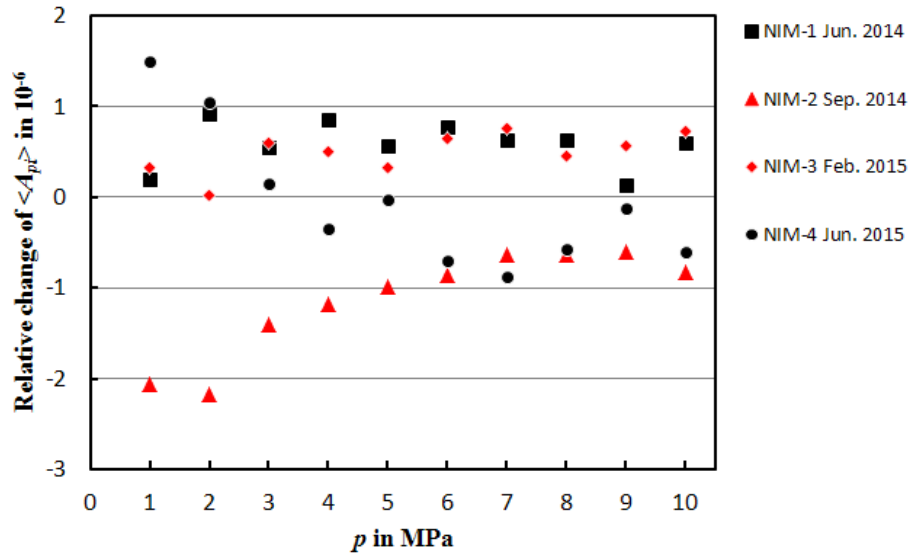
Figure 2. Relative changes of $\langle A_{pi} \rangle$

Figure 2 shows the relative changes of $\langle A_{pi} \rangle$ during the 4 calibrations. None unidirectional drift was observed. Assuming the variability shown in Figure 2 was random and complied normal distribution, the uncertainties due to long-term shift $u_{lts}(A_{pi})/A_{pi}$ can be estimated by a type B evaluation using equation (11) and are given in Table 12.

$$u_{lts}(A_{pi})/A_{pi} = \frac{1}{2} \frac{(A_{pi})_{\max} - (A_{pi})_{\min}}{A_{pi}} \quad (11)$$

Table 12. Uncertainty due to long-term shift at each pressure point

p in MPa	1	2	3	4	5	6	7	8	9	10
$u_{lts}(A_{pi})/A_{pi}$ in 10^{-6}	1.78	1.61	1.00	1.02	0.78	0.82	0.82	0.64	0.59	0.78

The combined uncertainties of A_{pi} for each laboratory were calculated from the root-sum-square of two component uncertainties, which are the relative standard uncertainty given in Table 7 and 8, and the uncertainty due to long-term shift given in Table 12.

$$u_c(A_{pi})/A_{pi} = \sqrt{[u(A_{pi})/A_{pi}]^2 + [u_{lts}(A_{pi})/A_{pi}]^2} \quad (12)$$

7. Results and discussions

7.1 Evaluation of degree of equivalence

The effective area A_{pi} and its combined uncertainty obtained by NIM and PTB are summarized in Table 13 and plotted in Figure 3. The average values in Figure 3 have been slightly shifted in abscissa for a better view.

Table 13. Comparison of results obtained by NIM and PTB

Nominal pressure	Average of A_{pi} , $\langle A_{pi} \rangle$ in mm^2		Combined uncertainty of A_{pi} , $u_c(A_{pi})/A_{pi}$ in 10^{-6}		
	MPa	NIM	PTB	NIM	PTB
1		98.04070	98.04183	12.4	6.8
2		98.04079	98.04181	11.0	5.8
3		98.04097	98.04190	10.7	5.5
4		98.04110	98.04195	10.7	5.4
5		98.04124	98.04205	10.8	5.4
6		98.04142	98.04212	11.0	5.4
7		98.04154	98.04222	11.2	5.4
8		98.04169	98.04231	11.4	5.3
9		98.04175	98.04240	11.7	5.3
10		98.04186	98.04247	12.0	5.4

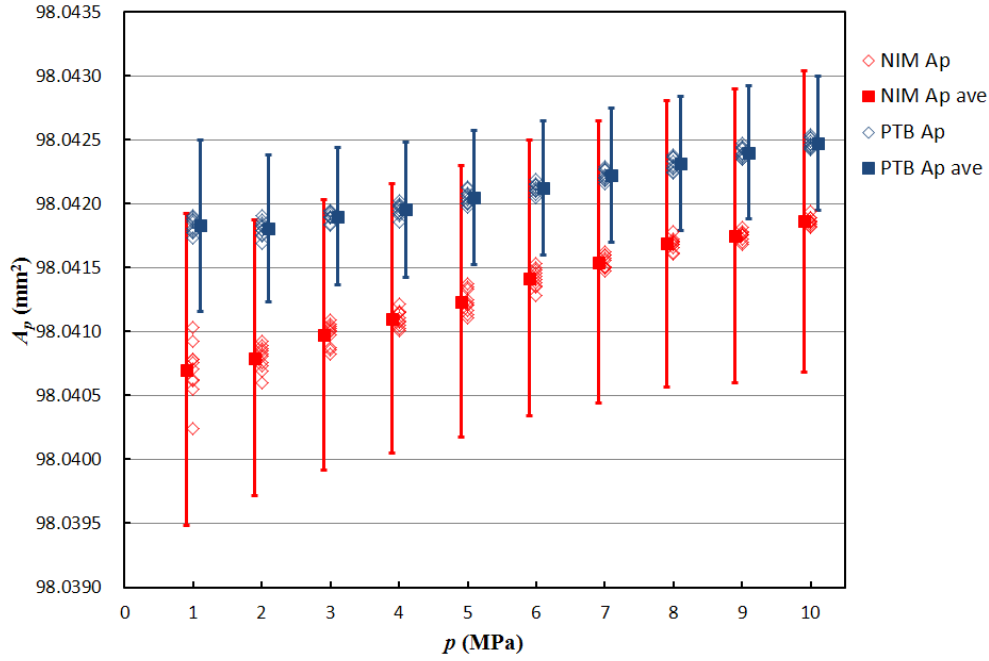


Figure 3. Measured effective areas and their average values with combined uncertainties ($k=1$) at each nominal pressure, NIM and PTB.

The degree of equivalence is expressed by the relative difference of the effective area between NIM and PTB at each nominal pressure (D_{p_i}) and the expanded uncertainty of this difference ($U(D_{p_i})$), which are calculated using equation (13) and (14). The normalized error (E_n) at each nominal pressure is calculated using equation (15). Table 14 presents the degree of equivalence between the LS of NIM and PTB based on these calculations.

$$D_{p_i} = \frac{A_{p_i, NIM}}{A_{p_i, PTB}} - 1 \quad (13)$$

$$U(D_{p_i}) = ku(D_{p_i}) = k \sqrt{\left(\frac{u_c(A_{p_i, NIM})}{A_{p_i, NIM}}\right)^2 + \left(\frac{u_c(A_{p_i, PTB})}{A_{p_i, PTB}}\right)^2}, \quad k=2 \quad (14)$$

$$E_n = \frac{|D_{p_i}|}{U(D_{p_i})} \quad (15)$$

Table 14. Degree of equivalence between the LS of NIM and PTB

Nominal pressure	Relative difference of A_{pi} between NIM and PTB, D_{pi}	Expanded uncertainty of D_{pi} , $U(D_{pi}) (k=2)$	E_n
MPa	10^{-6}	10^{-6}	
1	-11.5	28.4	0.41
2	-10.3	24.9	0.41
3	-9.4	24.1	0.39
4	-8.7	24.1	0.36
5	-8.3	24.2	0.34
6	-7.1	24.5	0.29
7	-7.0	24.9	0.28
8	-6.4	25.2	0.25
9	-6.6	25.7	0.26
10	-6.2	26.3	0.24

All the E_n values are below 0.5. That means the LS of NIM and PTB are equivalent even with a coverage factor of $k=1$.

7.2 Zero-pressure effective area and distortion coefficient

To determine the zero-pressure effective area of the TS (A_0) and its distortion coefficient (λ), model fit is calculated using the LINEST function in Excel based on all the reported effective areas $A_{p,i,j}$, where $i=1,2,\dots,10$, $j=1,2,\dots,10$, and total 100 data is used for each laboratory. The uncertainty of the fit (type A uncertainty) is calculated corresponding to the uncertainty of data distribution, which is $10 (\sqrt{100})$ times of the standard deviation obtained by the LINEST function. The uncertainty of the fit is combined with the type B uncertainty to calculate the uncertainty of A_0 and λ .

For the NIM data, a linear mode is used as expressed by equation (16), whereas model equation (17) is used for the PTB data

$$A_p = A_0(1 + \lambda p) \quad (16)$$

$$A_p = A_0(1 + \lambda p) + F/p \quad (17)$$

in which F presents a constant force correction. The fit results are summarized in Table 15.

Table 15. Results of A_0 and λ of TS and their uncertainties

	NIM			PTB		
	Value	Type A uncertainty	Combined Uncertainty	Value	Type A uncertainty	Combined Uncertainty
A_0 (mm ²)	98.04057	2.2×10^{-6} rel.	9.3×10^{-6} rel.	98.04154	2.5×10^{-6} rel.	5.7×10^{-6} rel.
λ (MPa ⁻¹)	1.37×10^{-6}	3.5×10^{-7}	7.1×10^{-7}	9.4×10^{-7}	3.0×10^{-7}	3.2×10^{-7}
F/g (mg)				19	33	37

The A_0 and λ of TS determined by NIM and PTB agree with each other within the claimed uncertainties. The E_n value for A_0 is 0.45, while it's 0.28 for λ .

A_0 calculated from each measured $A_{p_{i,j}}$ using the parameters as determined with the fit equation (16) and (17) are shown in Figure 4, together with the mean A_0 , its combined uncertainty and its expanded uncertainty ($k=2$).

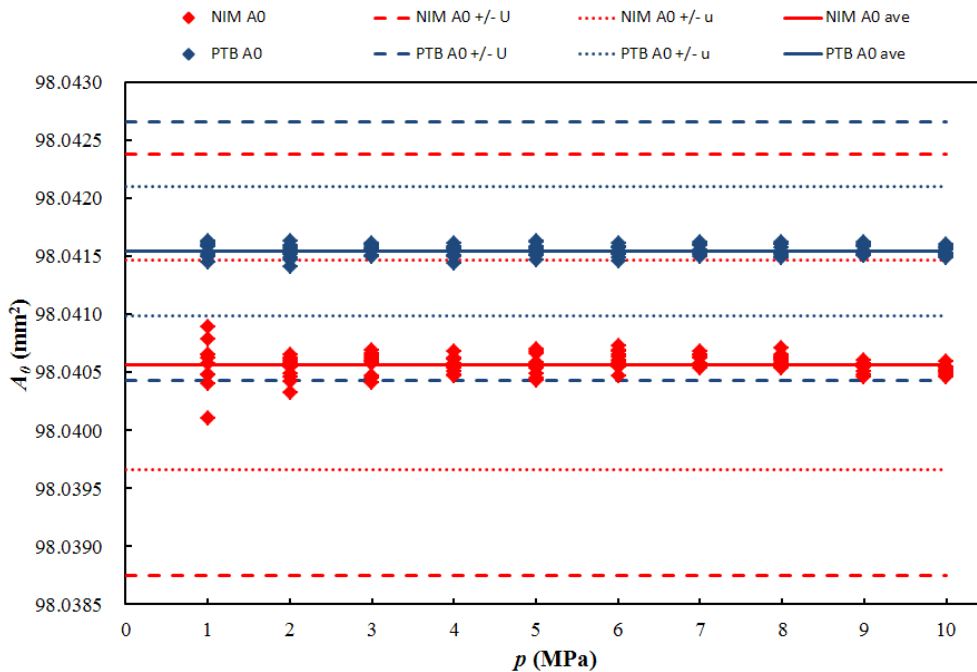


Figure 4. A_0 calculated from each measured $A_{p_{i,j}}$ together with the mean A_0 , its combined uncertainty and its expanded uncertainty ($k=2$) for NIM and PTB.

8. Conclusions and discussion

The relative difference of the effective areas determined by NIM and PTB varies from 6.2×10^{-6} to 11.5×10^{-6} , whereas the NIM values are lower than that of PTB. With the uncertainty claimed by each laboratory, the E_n values are in the range from 0.24 to 0.41, and all below 0.5, which means the LS of NIM and PTB are equivalent even with a coverage factor of $k=1$. The zero-pressure effective area and distortion coefficient of TS determined by NIM and PTB are also in agreement with each other within the claimed uncertainties.

The uncertainties claimed by NIM are about 2 times of that claimed by PTB. This is reasonable since the LS of PTB is a 5 cm^2 PCA whereas that of NIM is 1 cm^2 . With similar dimensional uncertainty, a larger PCA will result smaller uncertainty in the effective area.

Acknowledgements

The authors gratefully acknowledge Dr. Tokihiko Kobata (NMIJ, TCM chair of APMP) for assisting in registration of the comparison and transferring measurement data. Contributions of Mr. Thomas Konczak and Dr. Oliver Ott in carrying out and organizing the measurements at PTB are much appreciated. Contributions of Mr. Yinpeng Zhang in some measurements at NIM are acknowledged.

References

1. Yang Y., Yue J., Calculation of effective area for the NIM primary pressure standards, *PTB-Mitteilungen*, 2011, **121**(3): 266-269.
2. Jäger J., Schoppa G., Schultz W., The standard instruments of the PTB for the 1 GPa range of pressure measurement, *PTB-Report W-66*, Braunschweig, October 1996, ISSN 0947-7063, ISBN 3-89429-783-2.
3. Jäger J., Sabuga W., Wassmann D., Piston-cylinder assemblies of 5 cm^2 cross-sectional area used in an oil-operated primary pressure balance standard for the 10 MPa range, *Metrologia*, 1999, **36**(6): 541-544.
4. Sabuga W., Priruenrom T., An approach to synchronise effective areas of pressure balances, *MAPAN - Journal of Metrology Society of India*, 2014, DOI 10.1007/s12647-014-0116-y, http://link.springer.com/article/10.1007/s12647-014-0116-y?sa_campaign=email/event/articleAuthor/onlineFirst
5. Salama A.D., Sabuga W., Ulbig P., Measurement of the elastic constants of pressure balance materials using resonance ultrasound spectroscopy, *Measurement*, 2012, **45**: 2472-2475.
6. Sabuga W., Bergoglio M., Buonanno G., Legras J.C., Yagmur L., Calculation of the distortion coefficient and associated uncertainty of a PTB 1 GPa pressure balance using Finite Element

Analysis – EUROMET Project 463, *Proceedings of International Symposium on Pressure and Vacuum*, IMEKO TC16, Beijing, September 22-24, 2003, Acta Metrologica Sinica Press, 92-104.

7. Sabuga W., Molinar G., Buonanno G., Esward T., Legras J.C., Yagmur L., Finite element method used for calculation of the distortion coefficient and associated uncertainty of a PTB 1 GPa pressure balance – EUROMET project 463, *Metrologia*, 2006, **43**: 311-325.
8. Sabuga W., Determination of the pressure distortion coefficient of pressure balances using a modified experimental method, *Proceedings of NCSL International Workshop and Symposium*, San Diego, August 4-8 2002.
9. Technical Protocol of APMP of 10 MPa Hydraulic Gauge Pressure Bilateral Supplementary Comparison (APMP.M.P-S5), National Institute of Metrology (NIM), China, Edition 1.0 of 2014-04-30.
10. Giacomo P., Equation for the determination of the density of moist air, *Metrologia*, 1982, **18**: 33-40.
11. JCGM 100, GUM 1995 with minor corrections, Evaluation of measurement data - Guide to the expression of uncertainty in measurements, issued by BIPM, IEC, IFCC, ISO, IUPAC, IUPAP and OIML, 2008 (revised in 2010).